Available online at www.sciencedirect.com
ScienceDirect
Journal of Solid State Chemistry 181 (2008) 715–723
JOURNAL OF SOLID STATE CHEMISTRY
www.elsevier.com/locate/jssc

Structure and characterization of zero- to two-dimensional compounds built up of the sandwich-type clusters and transition-metal linkers

Zhiming Zhang[a], Shuang Yao[a], Enbo Wang[a,*], Chao Qin[a], Yanfei Qi[a], Yangguang Li[a,b,*], Rodolphe Clérac[b]

[a]*Key Laboratory of Polyoxometalate Science of Ministry of Education, Department of Chemistry, Northeast Normal University, Renmin Street No. 5268, Changchun, Jinlin 130024, PR China*
[b]*Université Bordeaux 1; CNRS, Centre de Recherche Paul Pascal (CRPP)-UPR 8641, 115 avenue du Dr. A. Schweitzer, 33600 Pessac, France*

Received 12 September 2007; received in revised form 14 December 2007; accepted 4 January 2008
Available online 19 January 2008

Abstract

Five new heteropolyoxotungstates $K_2Na_2Mn_2(H_2O)_{12}[Mn_2(H_2O)_{10}Mn_4(H_2O)_2(XW_9O_{34})_2]\cdot 18H_2O$ ($X=$ Ge, **1**; $X=$ Si, **2**), $Na_4[Mn_4(H_2O)_{18}Mn_4(H_2O)_2(XW_9O_{34})_2]\cdot 22H_2O$ ($X=$ Ge, **3**; $X=$ Si, **4**) and $K_3Na_5[Mn_2(H_2O)_6Mn_4(H_2O)_2(SiW_9O_{34})_2]\cdot 23.5H_2O$ (**5**) have been obtained by the routine synthetic reactions in aqueous solution. In **1** and **2**, two isolated Mn^{2+} ions are covalently linked to the sandwich-type polyoxoanions $[Mn_4(H_2O)_2(B\text{-}\alpha\text{-}XW_9O_{34})_2]^{12-}$ ($X=$ Ge or Si) by two μ_2-oxygen atoms resulting in the disupporting sandwich-type polyoxometalates (POMs). Compounds **3** and **4** are built from the disupporting sandwich-type polyoxoanions **1** and **2**, linked by additional four Mn^{2+} ions to construct a 1D ladder-like chain-like structure, which is rarely observed in the POM chemistry. Compound **5** represents the first example of the 2D structure consisting of the sandwich-type polyoxoanion $[Mn_4(H_2O)_2(SiW_9O_{34})_2]^{12-}$ and the binuclear $\{Mn_2(H_2O)_6\}^{4+}$ group. The magnetic studies of compounds **1**, **4** and **5** indicate that the antiferromagnetic interactions are predominant in the three compounds between Mn(II) metal ions.

Keywords: Manganese; Polyoxotungstate; Magnetism; Sandwich

1. Introduction

Polyoxometalates (POMs), as one kind of significant metal oxide cluster with nanosizes and abundant topologies, have been attracting extensive interest in fields such as catalysis, electrochemistry, electrochromism and magnetism [1,2]. The evolution of POMs chemistry is dependent upon the synthesis of novel polyoxoanions possessing unique structures and properties. POMs are formed by the early transition metals of groups V and VI in their highest oxidation states by condensation reactions in aqueous, acidic medium. Although the first POMs have been obtained 100 years ago, the mechanism of formation of POMs has not been well known up to now. The systemic synthesis of novel polyoxoanions is still a challenge in the POMs chemistry.

In the past decades, POMs were often used as building blocks to construct the 1D chain, 2D layer and 3D framework architectures with functional properties. To date, the commonly used POM building blocks still largely focus on the well-known Keggin- [3], Wells–Dawson- [4], Anderson- [5], Silverton- [6] and Lindquist-type [7] anions. Furthermore, the most extended frameworks based on these polyoxoanions are achieved via the bridges of metal-organic complexes [8]. Very recently, linking suitable metal oxide building blocks, such as the lacunary or transition-metal-substituted polyoxoanions, by simple metal cations as the bridging units to generate true metal oxide surfaces and framework materials has attracted considerable attention [9]. These kind of materials based on POM clusters have shown 1D chain-like structure by direct condensation to form oxo-bridged arrays of clusters or through metal cations acting as inorganic bridging ligands. However,

*Corresponding authors. Fax: +86 431 509 4009.
E-mail addresses: wangenbo@public.cc.jl.cn (E. Wang), Liyg658@nenu.edu.cn (Y. Li).

0022-4596/$ - see front matter © 2008 Elsevier Inc. All rights reserved.
doi:10.1016/j.jssc.2008.01.021

extended framework architectures based on the sandwich-type polyoxoanions have been rarely reported for POM chemistry [10].

The sandwich-type polyoxoanions, obtained by reaction of the lacunary polyoxoanions with the transition-metal cations, are the excellent building blocks [10]. Up to now, numerous sandwich-type polyoxoanions have been synthesized and mostly belong to the well-known Weakley-($[M_4(H_2O)_2(XW_9O_{34})_2]^{n-}$ and $[M_4(X_2W_{15}O_{56})_2]^{n-}$), Hervé-($[M_3(H_2O)_3(\alpha\text{-}XW_9O_{33})^2]^{n-}$ ($X = As^{III}$, Sb^{III}, Se^{IV}, Te^{IV}, Bi^{III})), Krebs- ($[M_2(H_2O)_6(WO_2)_2(\beta\text{-}XW_9O_{33})_2]^{n-}$) and Knoth-type ($[M_3(A\text{-}XW_9O_{34})_2]^{n-}$ ($X = P$ and Si)) sandwich-type structures [11–13]. They each accommodated a paramagnetic transition metal-set between two lacunary polyoxoanions. The introduction of central magnetic and electrochemical active metal-set leads to this class of polyoxoanions exhibiting interesting magnetic and electrochemical properties [14]. Incorporation of the sandwich polyoxoanions into an inorganic polymer will introduce the magnetic and electrochemical active centers into the extended structure and obtain the functional materials [10].

Inspired by the aforementioned considerations, we have attempted to study the systematic synthesis of extended structure based on the sandwich-type POMs. In this paper, we report the synthesis, structure and characterization of zero- to two-dimensional compounds built up of the sandwich-type $[Mn_4(H_2O)_2(B\text{-}\alpha\text{-}XW_9O_{34})_2]^{12-}$ ($X = Si$ and Ge) cluster covalently linked by the transition-metal cations.

2. Experimental section

2.1. General considerations

All chemicals were commercially purchased and used without further purification. $K_8[\gamma\text{-}SiW_{10}O_{36}]\cdot 12H_2O$, $K_8[\beta\text{-}SiW_{11}O_{39}]\cdot 14H_2O$, $K_8[\gamma\text{-}GeW_{10}O_{36}]\cdot 6H_2O$ and $K_8[\beta\text{-}GeW_{11}O_{39}]\cdot 14H_2O$ were synthesized according to the literature procedures [15] and characterized by IR spectra. Elemental analyses (H) were performed on a Perkin-Elmer 2400 CHN elemental analyzer; Si, Ge, W, Mn, Na and K were analyzed on a PLASMA-SPEC(I) ICP atomic emission spectrometer. IR spectra were recorded in the range 400–4000 cm^{-1} on an Alpha Centaurt FT/IR spectrophotometer using KBr pellets. TG analyses were performed on a Perkin-Elmer TGA7 instrument in flowing N_2 with a heating rate of 10 °C min^{-1}. Variable-temperature magnetic susceptibility data were obtained on a SQUID magnetometer (Quantum Design, MPMS-7) in the temperature range of 2–300 K with an applied field of 0.1 T.

2.2. Synthesis

2.2.1. Synthesis of *1*

In a typical synthesis procedure for **1**, $K_8[\beta\text{-}GeW_{11}O_{39}]\cdot 14H_2O$ (2.0 g, 0.61 mmol) was dissolved in 80 mL of distilled water with stirring. And then, 6 mL of 1 M $MnCl_2$ (6 mmol) solution was added dropwise with vigorously stirring and the mixture was boiled for 2 h. On stopping heating, 0.2 g NaN_3 (3.1 mmol) was added to the solution with stirring. After cooling to room temperature, the solution was filtered and the filtrate was slowly evaporated at room temperature for 3 days, resulting in a yellow block crystalline product (yield 51% based on Ge). Anal. Calcd. for **1** (%): K, 1.33; Na, 0.78; H, 1.50; Mn, 7.45; Ge, 2.46; W, 56.1. Found: K, 1.46; Na, 0.98; H, 1.39; Mn, 7.11; Ge, 2.16; W, 55.9. IR (KBr pellet): 941(m), 874(s), 768(s), 697(s), 511(m), 445(m) cm^{-1}.

2.2.2. Synthesis of *2*

The preparation of **2** was similar to that of **1** except that $K_8[\beta\text{-}SiW_{11}O_{39}]\cdot 14H_2O$ was used instead of $K_8[\beta\text{-}GeW_{11}O_{39}]\cdot 14H_2O$. Anal. Calcd. for **2** (%): K, 1.35; Na, 0.79; H, 1.47; Mn, 7.61; Si, 0.97; W, 57.3. Found: K, 1.53; Na, 0.93; H, 1.36; Mn, 7.36; Si, 1.11; W, 57.5. IR (KBr pellet): 944(m), 876(s), 720(s), 536(s), 513(m) cm^{-1}.

2.2.3. Synthesis of *3*

$K_8[\gamma\text{-}GeW_{10}O_{36}]\cdot 6H_2O$ (2.0 g, 0.69 mmol) was dissolved in 80 mL of distilled water with stirring. And then, 12 mL of 1 M $MnCl_2$ (12 mmol) solution, 0.3 g NaN_3 (4.6 mmol) and 6 mL 0.1 M $Nd(NO_3)_3$ (0.6 mmol) were added one by one with vigorously stirring and the mixture was boiled for 3 h. The solution was filtered the filtrate was kept at room temperature. Slow evaporation for 2 weeks resulted in the yellow block crystals (yield 32% based on Ge). Anal. Calcd. for **3** (%): Na, 1.58; H, 1.42; Mn, 7.56; Ge, 2.50; W, 56.9. Found: Na, 1.73; H, 1.56; Mn, 7.42; Ge, 2.39; W, 57.2. IR (KBr pellet): 937(m), 871(s), 767(s), 707(s), 511(m), 441(m) cm^{-1}.

2.2.4. Synthesis of *4*

$K_8[\gamma\text{-}SiW_{10}O_{36}]\cdot 12H_2O$ (2.0 g, 0.67 mmol) was dissolved in 80 mL of distilled water with stirring. And then, 12 mL of 1 M $MnCl_2$ (12 mmol) solution, 0.3 g NaN_3 (4.6 mmol) and 6 mL 0.1 M $Ce(NO_3)_3$ (0.6 mmol) were added one by one with vigorously stirring and the mixture was boiled for 3 h. The solution was filtered and the filtrate was kept at room temperature. Slow evaporation for half a month resulted in the yellow block crystals (yield 37% based on Si). Anal. Calcd. for **4** (%): Na, 1.60; H, 1.49; Mn, 7.64; Si, 0.98; W, 57.5. Found: Na, 1.86; H, 1.31; Mn, 7.45; Si, 1.05; W, 57.3. IR (KBr pellet): 946(s), 904(s), 873(s), 766(s), 517(s), 536(m), 407(m) cm^{-1}.

2.2.5. Synthesis of *5*

$K_8[\beta\text{-}SiW_{11}O_{39}]\cdot 14H_2O$ (1.5 g, 0.46 mmol) was dissolved in 50 mL of distilled water with stirring. And then, 5 mL of 1 M $MnCl_2$ (5 mmol) solution and 0.3 g NaN_3 (4.6 mmol) were added with vigorously stirring and the mixture was stirred for 10 h, and then the resulting solution is heated at 80 °C for 3 h. The solution was filtered and the filtrate was kept at room temperature. Slow evaporation for 5 weeks

resulted in the yellow block crystals (yield 21% based on Si). Anal. Calcd. for **5** (%): K, 2.10; Na, 2.06; H, 1.14; Mn, 5.90; Si, 1.01; W, 59.3. Found: K, 2.31; Na, 2.25; H, 1.21; Mn, 6.03; Si, 0.92; W, 59.1. IR (KBr pellet): 941(s), 908(s), 874(s), 725(s), 536(m), 514(m), 492(m) cm^{-1}.

2.3. X-ray crystallography

The yellow single crystals of compounds **1**–**5** with dimensions of $0.27 \times 0.21 \times 0.19$ (**1**), $0.26 \times 0.23 \times 0.19$ (**2**), $0.41 \times 0.37 \times 0.21$ (**3**), $0.40 \times 0.36 \times 0.22$ (**4**) and $0.33 \times 0.29 \times 0.21$ (**5**) mm were fixed to the end of a glass capillary, respectively. The measurements for the five compounds were performed on a Rigaku R-AXIS RAPID IP diffractometer. In all cases, the data were collected at 293 K, and graphite-monochromated Mo$K\alpha$ radiation ($\lambda = 0.71073$ Å) was used. Numerical absorption corrections were applied for compounds **1**–**5**. The structures were solved by the direct method and refined by the full-matrix least squares on F^2 using the SHELXL-97 software [16]. All hydrogen atoms for water molecules and protonation were not located, but were included in the structure factor calculations. The crystal data and structure refinements of compounds **1**–**5** are summarized in Table 1.

3. Results and discussion

3.1. Synthesis

Polyoxoanion $[\beta\text{-}SiW_{11}O_{39}]^{8-}$ decomposes easily in the aqueous solution, and, the divacant polyoxoanion $[\gamma\text{-}SiW_{10}O_{36}]^{8-}$ usually undergoes an isomerization course and decomposes in the aqueous solution [10f,14c,15a,15b]. Here, the two complexes are chosen to react with the Mn^{2+} ions, and three novel compounds **2**, **4** and **5** are obtained. Recently, the monovacant anion $[\beta\text{-}GeW_{11}O_{39}]^{8-}$ and another divacant polyoxoanion $[\gamma\text{-}GeW_{10}O_{36}]^{8-}$ are reported in the literature [15c]. Their structures and the synthetic procedures are essentially analogous to those of $[\beta\text{-}SiW_{11}O_{39}]^{8-}$ and $[\gamma\text{-}SiW_{10}O_{36}]^{8-}$, and, might possess similar reactivity with Si analogs $[\beta\text{-}SiW_{11}O_{39}]^{8-}$ and $[\gamma\text{-}SiW_{10}O_{36}]^{8-}$ when reacted with transition-metal cations or other electrophiles. Here, the two polyoxoanions were used to react with the Mn^{2+} ions and obtained compounds **1** and **3**, respectively. The successful synthesis of both compounds **1** and **3** can prove that $[\beta\text{-}GeW_{11}O_{39}]^{8-}$ and $[\gamma\text{-}GeW_{10}O_{36}]^{8-}$ anions might possess similar reactivity with Si analogs $[\beta\text{-}SiW_{11}O_{39}]^{8-}$ and $[\gamma\text{-}SiW_{10}O_{36}]^{8-}$ when reacted with transition-metal cations. But no isostructural compound of **5** was obtained under these conditions. Additionally, the presence of the azido ligand during the synthetic process seems crucial. In the absence of the NaN_3, only the $[Mn_4(H_2O)_2(B\text{-}\alpha\text{-}XW_9O_{34})_2]^{12-}$ (X = Si and Ge) polyoxoanions are obtained in the synthetic procedures of compounds **3** and **4**. If the NaN_3 was replaced by the same concentration NaCl or NaBr in the synthetic procedure of the five compounds, also the polyoxoanions $[Mn_4(XW_9O_{34})_2]$ (X = Si and Ge) are obtained in the synthetic procedures of compounds **3** and **4**. Accordingly, the N_3^- is significant for the formation of the five title compounds, but the role of this N_3^- ligand remains unclear.

Table 1
Crystal data and structure refinement for compounds **1**–**5**

	1	**2**	**3**	**4**	**5**
Empirical formula	$H_{84}Ge_2K_2Mn_8Na_2O_{110}W_{18}$	$H_{84}K_2Mn_8Na_2O_{110}Si_2W_{18}$	$H_{84}Ge_2Mn_8Na_4O_{110}W_{18}$	$H_{84}Mn_8Na_4O_{110}Si_2W_{18}$	$H_{63}K_3Mn_6Na_5O_{99.5}Si_2W_{18}$
Formula mass	5862.85	5773.85	5830.63	5741.63	5582.87
Temperature (K)	293(2)	293(2)	293(2)	293(2)	293(2)
Wavelength (Å)	0.71073	0.71073	0.71073	0.71073	0.71073
Crystal system	Monoclinic	Monoclinic	Triclinic	Triclinic	Triclinic
Space group	$P2_1/n$	$P2_1/n$	$p\bar{1}$	$p\bar{1}$	$p\bar{1}$
a (Å)	17.751(4)	17.686(4)	12.477(3)	12.503(3)	12.373(3)
b (Å)	12.126(2)	12.128(2)	13.357(3)	13.296(3)	13.746(3)
c (Å)	22.541(5)	22.504(5)	16.830(3)	16.862(3)	15.464(3)
α (deg)	90	90	103.37(3)	103.28(3)	70.69(3)
β (deg)	95.50(3)	95.42(3)	103.34(3)	103.26(3)	79.46(3)
γ (deg)	90	90	111.97(3)	112.13(3)	69.61(3)
V (Å^3)	4829.6(17)	4805.2(17)	2369.1(8)	2366.8(8)	2319.8(8)
Z	2	2	1	1	1
D_{calcd} (g cm^{-3})	4.032	3.991	4.087	4.028	3.996
μ (mm^{-1})	23.177	22.706	23.545	22.970	23.302
$F000$	5240	5168	2604	2568	2481
R_1[a] [$I > 2\sigma(I)$]	0.0479	0.0429	0.0634	0.0467	0.0553
wR_2[b]	0.1060	0.0931	0.1288	0.1018	0.1189

[a] $R_1 = \sum||F_o|-|F_c||/\sum|F_o|$.
[b] $wR_2 = \sum[w(F_o^2-F_c^2)^2]/\sum[w(F_o^2)^2]^{1/2}$.

3.2. Structure description

3.2.1. Structural analysis of *1* and *2*

Single-crystal X-ray diffraction analyses reveal that compounds **1** and **2** are isostructural, and the unit cell dimensions, volumes, related bond distances and angles are only slightly changed, which are all composed of a disupporting sandwich-type polyoxoanion $[Mn_2(H_2O)_{10}Mn_4(H_2O)_2(XW_9O_{34})_2]^{8-}$, two counter $[Mn(H_2O)_6]^{2+}$ groups, two K^+ ions, two Na^+ ions and 18 lattice water molecules. Fig. 1a and b are the ball-and-stick and the polyhedral representations of the polyoxoanions **1** and **2**. In each compound, the anion is composed of two isolated Mn^{2+} ions and a sandwich-type polyoxoanion $[Mn_4(H_2O)_2(B\text{-}\alpha\text{-}XW_9O_{34})_2]^{12-}$ (X = Ge or Si). In the two compounds, the well-known sandwich-type polyoxoanion consists of two trivacant $[B\text{-}\alpha\text{-}XW_9O_{34}]^{10-}$ (X = Ge and Si) Keggin moieties sandwiching a central symmetric rhomb-like $Mn_4(H_2O)_2$ segment via the W–O–Mn and X–O–Mn connecting modes. All the W and Mn centers exhibit the octahedral coordination environments. The bond lengths of W–O are in the range of 1.688(10)–2.399(9) Å in **1** and 1.703(10)–2.441(10) Å in **2**, while the bond lengths of Mn–O are in the range of 2.095(9)–2.23(2) Å in **1** and 2.099(11)–2.241(9) in **2**. It is noteworthy that two Mn^{2+} cations are coordinated directly to the surface oxygen atoms of the sandwich-type polyoxoanion resulting in a disupporting sandwich-type polyoxoanion (see Fig. 1), which is reported for the first time in the Mn-containing POMs. The structure of the title polyoxoanions is similar to the Cu-substituted As-containing polyoxoanion $[\{Cu(\beta\text{-Ala})_2(H_2O)_2\}_2Cu_4(H_2O)_2(B\text{-}\alpha\text{-}AsW_9O_{34})_2]^{6-}$ [17]. In the Cu-substituted polyoxoanion, the isolated Cu^{2+} ions are coordinated to two β-Ala molecules to form the $\{Cu(\beta\text{-Ala})_2(H_2O)_2\}$ complex which is associated with the sandwich-type polyoxoanion $[Cu_4(H_2O)_2(B\text{-}\alpha\text{-}AsW_9O_{34})_2]^{10-}$ by weak covalent interaction.

Interestingly, the disupporting sandwich-type polyoxoanions are connected by the K^+ ions into a 2D framework (Fig. 2). In the 2D framework, the K^+ ion is in an eight-coordinate environment and coordinated to four bridging oxo-groups of one $[Mn_4(H_2O)_2(XW_9O_{34})_2]^{12-}$ cluster, two terminal oxygen atoms from another two neighboring $[Mn_4(H_2O)_2(XW_9O_{34})_2]^{12-}$ clusters and two water molecules (Fig. S1). Thus, the potassium cations can be viewed as μ_3-bridges and each of them links with three polyoxoanion moieties resulting in a 2-D porous layer (Fig. 2). The bond lengths of K–O are in the range of 2.761 (11)–2.955 (10) Å in **1** and 2.738(11)–2.965(11) Å in **2**.

3.2.2. Structural analysis of *3* and *4*

The single-crystal X-ray diffraction analyses reveal that compounds **3** and **4** are isostructural and crystallize in the same space group $P\bar{1}$, therefore, we only discuss the structure of **3** herein. The crystal structure of **3** is a polymeric chain $[Mn_4(H_2O)_{18}Mn_4(H_2O)_2(GeW_9O_{34})_2]_n^{4n-}$, constructed from the sandwich anions $[Mn_4(H_2O)_2(GeW_9O_{34})_2]^{12-}$ and the Mn^{2+} ions (Fig. 3). In this polymeric chain, two Mn^{2+} linkers coordinate to a sandwich-type anion by two μ_2-O atoms and link the neighboring anion to constitute the 1D ladder-like chain (Fig. 3), which represents the first example of the 1D ladder-like chain based on the sandwich-type anions and the transition-metal linkers. Additionally, another two Mn^{2+} ions coordinated to the sandwich-type polyoxoanion and form a 10-Mn^{2+}-containing unit (Fig. 4). To our

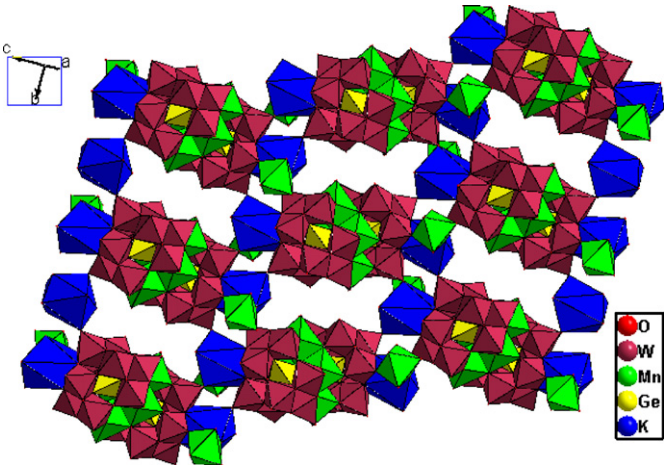

Fig. 2. View of the 2-D framework structure of compound **1**.

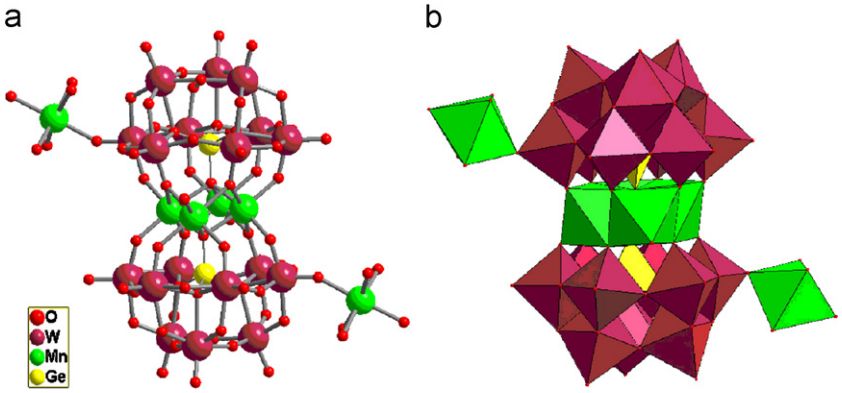

Fig. 1. (a) Ball-and-stick representation of polyoxoanion **1** and (b) polyhedral representation of polyoxoanion **1**.

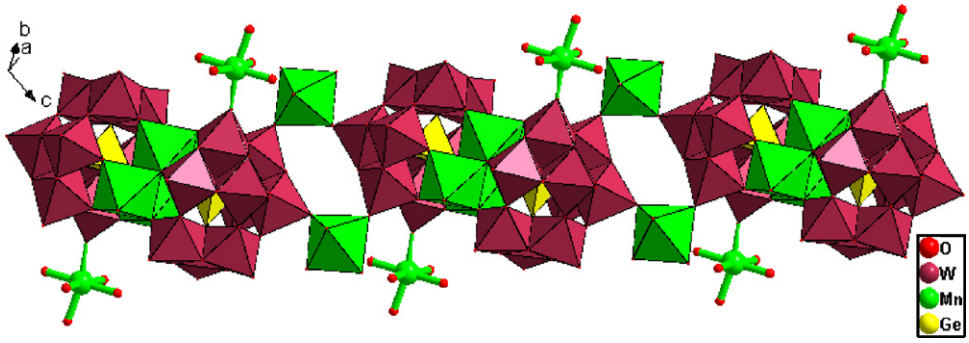

Fig. 3. View of the 1-D ladder-like chain in **3**.

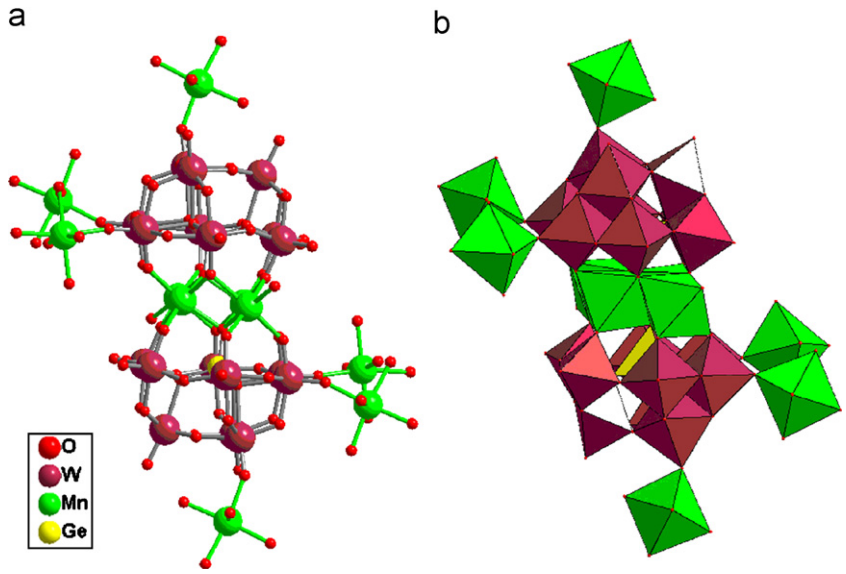

Fig. 4. (a) Ball-and-stick representation of sandwich-type polyoxoanion coordinated by the Mn^{2+} ions in **3** and (b) polyhedral representation of the sandwich-type polyoxoanion coordinated by the Mn^{2+} ions in **3**.

knowledge, this is the first sandwich-type polyoxoanion coordinated to six transition-metal cations. Alternatively, the polymeric chain in **3** can be regarded as an aggregate consisting of the disupporting sandwich-type polyoxoanion **1**, connected together by four Mn^{2+} ions to constitute the 1D ladder-like chain.

Interestingly, polymeric chains $[Mn_4(H_2O)_{18}Mn_4(H_2O)_2(GeW_9O_{34})_2]_n^{4n-}$ are linked by the binuclear $Na_2(H_2O)_8$ group into a 2D framework. Within the 2D framework, the $Na_2(H_2O)_8$ group, built up of two edge-sharing NaO_6 octahedral, is connected with two $[Mn_4(H_2O)_2(GeW_9O_{34})_2]^{12-}$ clusters, derived from two neighboring polymeric chains, via two terminal-oxo atoms to constitute the 2D framework (Fig. 5). Generally, sodium cations and water molecules in the heteropolyanion complexes are crystallography problematical to be distinguished. As mentioned by Zhang et al. [10b], the location of the linking sodium cations at the crystallographic special position in compounds **3** and **4** is unambiguous on the basis of the four criteria: (i) its peak height in the difference Fourier map, (ii) its coordination geometry, (iii) the refinement results, and (iv) the consistency in two different structure determinations of compounds. The lengths of the Na1–O26 and W2–O26 bonds that define the linkages between the polyoxoanions are 2.280(15) and 1.699(15) Å in **3**, 2.256(13) and 1.716(11) Å in **4**, respectively, and the Na1–O distances fall in the range of 2.15(2)–2.55(3) Å in **3** and 2.117(16)–2.60(3) Å in **4**.

3.2.3. *Structural analysis of* **5**

The structure of **5** is composed of sandwich-type $[Mn_4(H_2O)_2(SiW_9O_{34})_2]^{12-}$ anionic moieties, dimeric $\{Mn_2(H_2O)_6\}^{4+}$ complex, K^+ cations, Na^+ cations and lattice water molecules. As shown in Fig. 6, compound **5** shows a 2D structure constructed by the anion $[Mn_4(H_2O)_2(SiW_9O_{34})_2]^{12-}$ and the binuclear $\{Mn_2(H_2O)_6\}^{4+}$ group. In the 2D framework, the Weakley-type polyoxoanion $[Mn_4(H_2O)_2(SiW_9O_{34})_2]^{12-}$, which has been reported previously and also observed in the compounds **1** and **4**, is covalently bonded to four adjacent $\{Mn_2(H_2O)_6\}^{4+}$ clusters via four terminal-oxo atoms, and each $\{Mn_2(H_2O)_6\}^{4+}$ cluster, composed of two edge-sharing

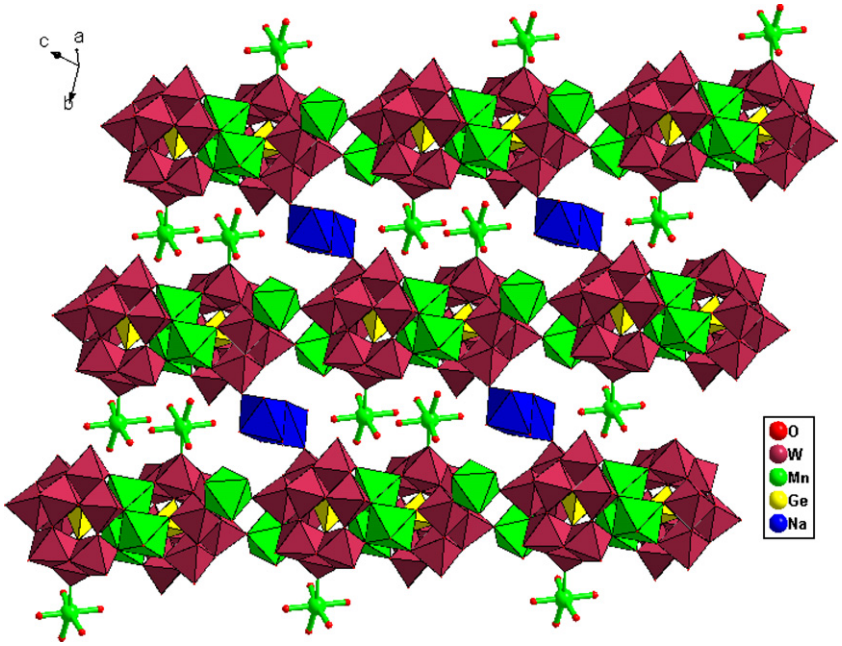

Fig. 5. View of the 2-D framework structure of compound **3**.

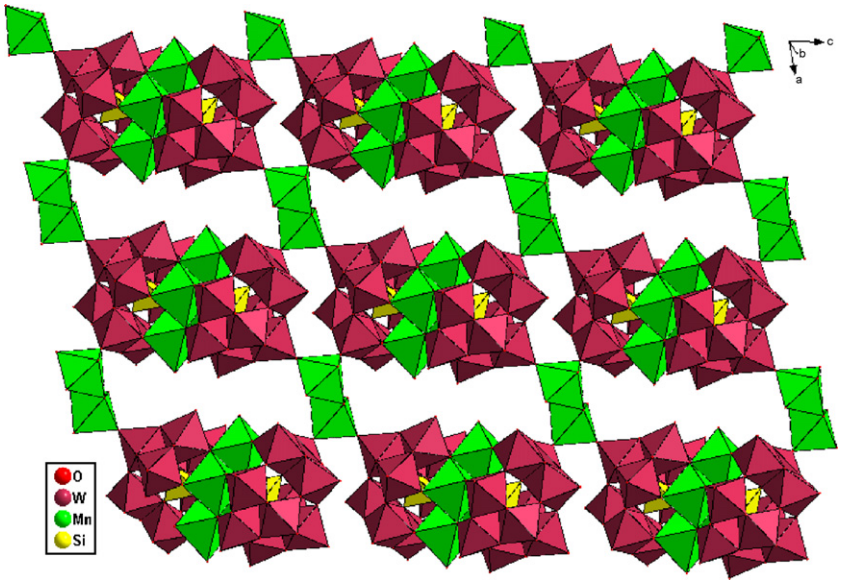

Fig. 6. View of the 2-D framework structure of compound **5** constructed by the sandwich-type polyoxoanions and $Mn_2(H_2O)_6$ cluster.

MnO_6 octahedral, is connected with four $[Mn_4(H_2O)_2(SiW_9O_{34})_2]^{12-}$ clusters to constitute the 2D framework (Fig. 6), which represents the first example of the 2D framework constructed from the sandwich-type polyoxoanions and the binuclear transition-metal $\{Mn_2(H_2O)_6\}^{4+}$ groups. The Mn–O distances in the $\{Mn_2(H_2O)_6\}^{4+}$ group fall into the rational range of 2.09(2)–2.232(18) Å. It is noteworthy that there are four binuclear $Na_2(H_2O)_8$ groups and two K^+ ions distributed around every $[Mn_4(H_2O)_2(SiW_9O_{34})_2]^{12-}$ cluster in the 2D framework. Each of the binuclear $Na_2(H_2O)_8$ group is coordinated to two terminal oxygen atoms of two adjacent anions and eight lattice water molecules, and they linked the $[Mn_4(H_2O)_2(SiW_9O_{34})_2]^{12-}$ cluster to constitute a 1D chain-like structure along the *a*-axis (Fig. S2). The linking K^+ (K1) ion in the 2D structure is coordinated to eight bridging oxo-groups of two neighboring $[Mn_4(H_2O)_2(SiW_9O_{34})_2]^{12-}$ clusters (Fig. S3) and connected the $[Mn_4(H_2O)_2(SiW_9O_{34})_2]^{12-}$ clusters into a 1D chain-like structure along the *c*-axis. The Na–O distances fall in the range of the 2.24(4)–2.82(4) Å and the bond lengths of K–O are in the range of 2.853(12)–2.924(15) Å. The two 1D chain-like structures are arranged perpendicularly to constitute the 2D structure (Fig. S2). Another interesting feature of compound **5** is that the 2D layers are connected together by additional $K2^+$ ions into a 3D open framework (Fig. 7).

The coordination geometry of $K2^+$ is octahedral (Fig. S3) and the K–O distances fall into the range of 2.62(4)–2.932(18) Å.

The oxidation states of W and Mn sites in the five compounds are determined based on the crystal color, bond lengths and angles, charge balance consideration and bond valence sum calculation [18], indicating that all W and Mn sites possess +6 and +2 oxidation states, respectively (the selected bond lengths of compounds **1**–**5** are listed in Table S1). Bond valence sum calculation [18] also reveals that bridging oxygen atoms linking two adjacent manganese ions and the terminal oxygen atoms associated to the manganese ions in the five compounds are all diprotonated.

3.3. Magnetic properties

The magnetic properties of compounds **1**, **4** and **5** have been studied at 1000 Oe between 1.8 and 300 K on polycrystalline samples and also performed on single crystals, and the results are consistent with those of polycrystalline power samples. It is worth mentioning that these three compounds possess a common $[Mn_4^{II}]$ core (inset of Fig. 8) with four additional isolated Mn(II) ions for **1** and **4** and a dinuclear $[Mn_2]$ unit in **5**. In order to compare their magnetic behaviors, the data for compounds **1** and **4** will be presented per six Mn(II) metals ions by removing the Curie contribution of two isolated Mn(II) ions. The resulting three sets of data are shown in Fig. 8. At a first look, it is worth remarking that the magnetic behavior of these compounds is extremely similar. At room temperature, the χT values are equal to 24.8 $cm^3\,K\,mol^{-1}$ and continuously decrease down to 6.5 $cm^3\,K\,mol^{-1}$ at 1.8 K revealing the presence of dominant antiferromagnetic interactions between Mn(II) $S = 5/2$ magnetic centers. For

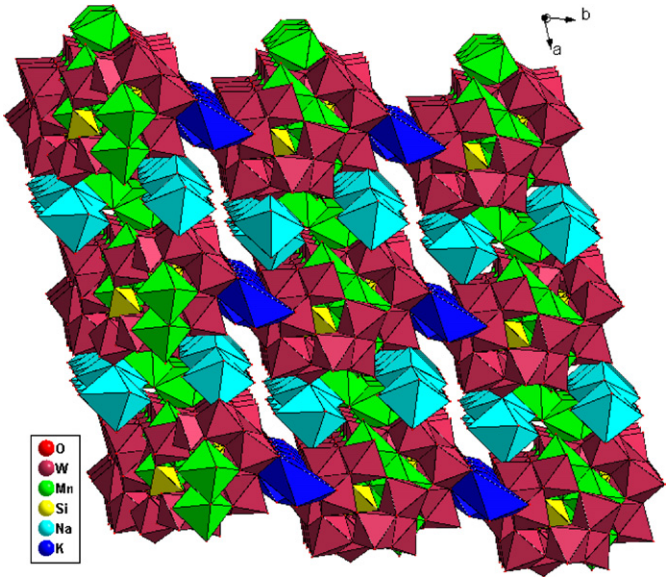

Fig. 7. View of the 3-D framework structure of compound **5**.

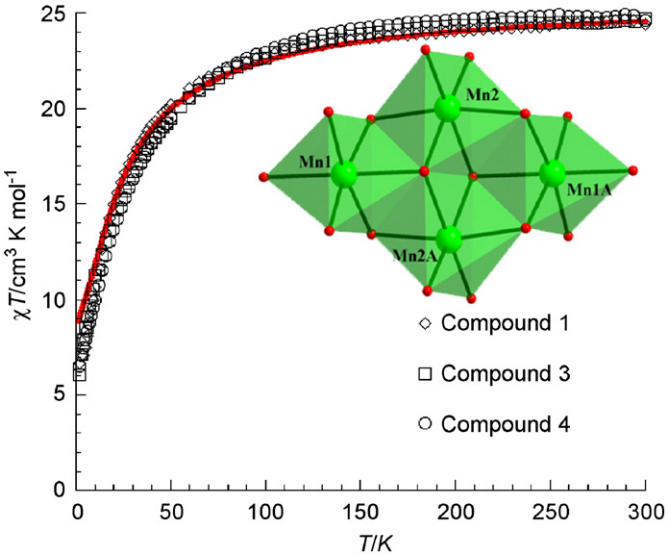

Fig. 8. The temperature dependence of the product χT (where $\chi = M/H$) of a polycrystalline sample of **1**, **4** and **5** at 1000 Oe.

the three compounds the data obey a Curie–Weiss law above 20 K leading to Curie constants of 25.7, 26.4 and 26.9 $cm^3\,K\,mol^{-1}$ and Weiss constants of −13.8, −17.6 and −19.1 K for **1**, **4** and **5**, respectively. The Curie constants are well in agreement with the expected value for six Mn^{2+} centers ($C = 26.25\,cm^3\,K\,mol^{-1}$ assuming $g = 2.0$). The Weiss constants confirm the presence of antiferromagnetic interactions between the Mn^{2+} $S = 5/2$ spins, but also show that their amplitude is roughly the same in the three compounds. Indeed similar magnetic behaviors have been observed in the other polyoxoanions containing the $[Mn_4^{II}O_{14}(H_2O)_2]$ cluster [10d,19]. Therefore the same numerical approach [20] has been used in order to model the magnetic susceptibility for compounds **1** and **4**, considering, moreover, that the additional Mn(II) metal ions are uncoupled to the central $[Mn_4]$ core. Concerning **5**, the similarity of its magnetic behavior with the two other compounds suggests that the magnetic interaction in the additional $[Mn_2]$ motif is very small and that these Mn(II) spins can be considered isolated at least above 15 K in the temperature region of the simulation described below. Therefore, the susceptibility was simulated considering the following isotropic Heisenberg spin Hamiltonian:

$$H = -2J_{wb}((S_1 + S_2)(S_3 + S_4)) - 2J_{bb}(S_1S_2),$$

where S_i are the spin operators for each metal ions ($S_i = 5/2$ for Mn^{II} with $i = 1$–4), J_{bb} and J_{wb} the magnetic interaction between the two central Mn(II) sites and between central Mn(II) and external Mn(II) spins. This simulation procedure (including a Curie contribution for the two isolated Mn(II) metal ions) is working well down to 15 K (red line in Fig. 8) for the three compounds with $g = 1.97(2)$, $J_{wb}/k_B = -1.7(3)$ K and is really independent of the value of J_{bb}/k_B as long as it ranges between −0.5 and +2 K. It is worth mentioning that other values of J_{bb}/k_B

do not improve the quality of the simulation below 15 K. Even if our data do not allow us to determine J_{bb} accurately (noting that the ground state of the [Mn_4] unit does not change and it is still in all cases $S_T = 0$), it is important to mention that the J_{wb} interaction values obtained are in good agreement with the previous reports on similar system [19]. Below 15 K, the magnetic properties of these systems are probably influenced by the presence of additional inter-unit magnetic interactions between the Mn(II) metal ions that have not been considered in our model. This hypothesis is reinforced by the χT value at 1.8 K (6.5 $cm^3 K mol^{-1}$) that is much smaller than the value expected for two isolated Mn(II) metal ions (8.75 $cm^3 K mol^{-1}$).

3.4. FT-IR spectroscopy and TG analyses

In the IR spectrum of compound **1**, the features at 941(m), 874(s), 768(s), 697(s), 511(m), 445(m) cm^{-1} can be attributed to ν(W–Od), ν(Ge–Oa), ν(W–Ob) and ν(W–Oc) of the polyoxoanion (Fig. S4). The IR spectra of compounds **2**–**5** are similar to that of **1** (see Figs. S4–S8). The characteristic peaks in the IR spectra of the four compounds are located at: 944(m), 876(s), 720(s), 536(s), 513(m) cm^{-1} for **2**, 937(m), 871(s), 767(s), 707(s), 511(m), 441(m) cm^{-1} for **3**, 946(s), 904(s), 873(s), 766(s), 517(s), 536(m), 407(m) cm^{-1} for **4** and 941(s), 908(s), 874(s), 725(s), 536(m), 514(m), 492(m) cm^{-1} for **5**.

In order to examine the thermal stability of compounds **1**–**5**, thermal gravimetric (TG) analyses were carried out for the five compounds. TG curve of **1** (Fig. S9) shows two continuous weight loss steps from 28 to 400 °C, attributed to the loss of all lattice and coordinated water molecules in **1**. The total weight loss is about 10.51%, which is a little lower than the calculated value of 12.89%. The TG curve of compound **2** is similar to that of compound **1** (Fig. S10). The weight loss is about 10.85% (calculated value 13.09).

TG curve of **3** shows a weight loss of 12.31% in the range of 30–350 °C (calcd. 12.97%), which corresponds to the loss of all non-coordinated and coordinated water molecules (Fig. S11), and the TG curve of compound **4** is similar to that of compound **3** (Fig. S12). The weight loss is about 12.78% (calculated value 13.17).

TG curve of **5** is shown in Fig. S13 and gives a total weight loss of 9.98% in the temperature range of 35–570 °C (calculated value of 10.16%), which corresponds to the loss of all non-coordinated and coordinated water molecules in compound **5**.

4. Conclusions

In conclusion, five new heteropolyoxotungstates $K_2Na_2Mn_2(H_2O)_{12}[Mn_2(H_2O)_{10}Mn_4(H_2O)_2(XW_9O_{34})_2]\cdot 18H_2O$ (X = Ge, **1**; X = Si, **2**), $Na_4[Mn_4(H_2O)_{18}Mn_4(H_2O)_2(XW_9O_{34})_2]\cdot 22H_2O$ (X = Ge, **3**; X = Si, **4**) and $K_3Na_5[Mn_2(H_2O)_6Mn_4(H_2O)_2(SiW_9O_{34})_2]\cdot 23.5H_2O$ (**5**), from zero- to two-dimensional built up of the sandwich-type clusters and transition-metal linkers, have been obtained in the aqueous solution, and their structures were determined by X-ray single-crystal diffraction analysis. Compounds **1** and **2** are the disupporting sandwich-type POMs and are connected together by K^+ ions to constitute the 2D structure. The polyoxoanion frameworks of **3** and **4** are built from the disupporting sandwich-type POMs **1** and **2**, covalently linked by additional Mn^{2+} ions to construct the 1D ladder-like chain-like structure, which is observed firstly in the POMs chemistry. Furthermore, polymeric chains are linked together by the binuclear $Na_2(H_2O)_8$ group into a 2D framework. Compound **5** shows a 2D structure consisting of the anion $[Mn_4(H_2O)_2(SiW_9O_{34})_2]$ and the binuclear $\{Mn_2(H_2O)_6\}^{4+}$ group, which represents the first example of 2D structure based on the Mn-containing sandwich-type polyoxoanion. Future research will focus on the synthesis of inorganic congregates based on other transition-metal-substituted sandwich-type polyoxoanions. The subsequent synthesis of 2D and 3D organic–inorganic hybrid materials, with the introduction of magnetic and electrochemically active centers could open the way to new functional materials.

Supplementary materials

TG and IR spectra, view of the coordination environments of potassium cations in compounds **1**, **2** and **5**, selected bond lengths of the five compounds and additional figures, X-ray crystallographic information files (CIF) are available for compounds **1**–**5**. Further details on the crystal structure investigations may be obtained from the Fachinformationszentrum Karlsruhe, 76344 Eggenstein-Leopoldshafen, Germany (fax: (+49)7247-808-666; e-mail: crysdata@fiz-karlsruhe.de), on quoting the depository numbers CSD-418116 for **1**, CSD-418117 for **2**, CSD-418118 for **3**, CSD-418119 for **4** and CSD-418120 for **5**.

Acknowledgments

This work was supported by the National Natural Science Foundation of China (20701005/20701006); Science and Technology Development Project Foundation of Jilin Province (20060420); Analysis and testing foundation of Northeast Normal University; Ph.D. station Foundation of Ministry of Education (20060200002); Science Foundation for Young Teachers of Northeast Normal University (No. 20070302/20070312); Science and Technology Creation Foundation of Northeast Normal University (NENU-STC07009); the Bordeaux 1 University; the CNRS and the "Région Aquitaine".

Appendix A. Supplementary information

Supplementary data associated with this article can be found in the online version at doi:10.1016/j.jssc.2008.01.021.

References

[1] (a) M.T. Pope, Heteropoly and Isopoly Oxometalates, Springer, Berlin, 1983;
(b) J.S. Anderson, Nature 140 (1937) 850;
(c) H.T. Evans Jr., J. Am. Chem. Soc. 70 (1948) 1291;
(d) K. Fukaya, T. Yamase, Angew. Chem. Int. Ed. 42 (2003) 654;
(e) P. Mialane, A. Dolbecq, F. Sécheresse, Chem. Commun. (2006) 3477.

[2] (a) C.L. Hill, Chem. Rev. 98 (1998) 1;
(b) B.B. Xu, Z.H. Peng, Y.G. Wei, D.R. Powell, Chem. Commun. (2003) 2562;
(c) L.C. Baker, D.C. Glick, Chem. Rev. 98 (1998) 3;
(d) E. Coronado, C.J. Gómez-García, Chem. Rev. 98 (1998) 273;
(e) D.L. Long, E. Burkholder, L. Cronin, Chem. Soc. Rev. 36 (2007) 105;
(f) Z.M. Zhang, E.B. Wang, Y.F. Qi, Y.G. Li, B.D. Mao, Z.M. Su, Cryst. Growth Des. 7 (2007) 1305.

[3] (a) M. Sadakane, M.H. Dickman, M.T. Pope, Angew. Chem. Int. Ed. 39 (2000) 2914;
(b) J.M. Galan-Mascaros, C. Gimenez-Saiz, S. Triki, C.J. Gomez-Garcia, E. Coronado, L. Ouahab, Angew. Chem. Int. Ed. Engl. 34 (1995) 1460;
(c) A. Müller, M. Koop, P. Schiffels, H. Bögge, Chem. Commun. (1997) 1715;
(d) H.Y. An, E.B. Wang, D.R. Xiao, Y.G. Li, Z.M. Su, L. Xu, Angew. Chem. Int. Ed. 45 (2006) 904;
(e) X.L. Wang, C. Qin, E.B. Wang, Z.M. Su, Y.G. Li, L. Xu, Angew. Chem. Int. Ed. 45 (2006) 1.

[4] (a) J.Y. Niu, D.J. Guo, J.P. Wang, J.W. Zhao, Cryst. Growth Des. 5 (2005) 837;
(b) Y. Lu, Y. Xu, Y.G. Li, E.B. Wang, X.X. Xu, Y. Ma, Inorg. Chem. 5 (2006) 2055.

[5] (a) V. Shivaiah, P.V. Reddy, L. Cronin, S.K. Das, J. Chem. Soc. Dalton Trans. (2002) 3781;
(b) H.Y. An, Y.G. Li, E.B. Wang, D.R. Xiao, C.Y. Sun, L. Xu, Inorg. Chem. 17 (2005) 6062;
(c) H.Y. An, Y.G. Li, D.R. Xiao, E.B. Wang, C.Y. Sun, Cryst. Growth Des. 5 (2006) 1107.

[6] C.D. Wu, C.Z. Lu, H.H. Zhuang, J.S. Huang, J. Am. Chem. Soc. 124 (2002) 3836.

[7] P.J. Hagrman, D. Hagrman, J. Zubieta, Angew. Chem. Int. Ed. 38 (1999) 3165.

[8] (a) C.M. Liu, D.Q. Zhang, D.B. Zhu, Cryst. Growth Des. 5 (2005) 1639;
(b) Y. Lu, Y. Xu, E.B. Wang, J. Lu, C.W. Hu, L. Xu, Cryst. Growth Des. 5 (2005) 257;
(c) M. Liu, D.Q. Zhang, M. Xiong, D.B. Zhu, Chem. Commun. (2002) 1416.

[9] (a) M.I. Khan, E. Yohannes, D. Powell, Chem. Commun. (1999) 23;
(b) M.I. Khan, E. Yohannes, J.R. Doedens, Angew. Chem. Int. Ed. 38 (1999) 1292;
(c) X.B. Cui, J.Q. Xu, H. Meng, S.T. Zheng, G.Y. Yang, Inorg. Chem. 43 (2004) 8005.

[10] (a) J.P. Wang, X.D. Du, J.Y. Niu, Chem. Lett. 35 (2006) 1408;
(b) X. Zhang, Q. Chen, D.C. Duncan, C.F. Campana, C.L. Hill, Inorg. Chem. 36 (1997) 4208;
(c) S.T. Zheng, D.Q. Yuan, J. Zhang, G.Y. Yang, Inorg. Chem. 46 (2007) 4569;
(d) U. Kortz, S. Nellutla, A.C. Stowe, N.S. Dalal, J. Tol, B.S. Bassil, Inorg. Chem. 43 (2004) 144;
(e) C. Ritchie, E.M. Burkholder, D.L. Long, D. Adam, P. Kögerlerb, L. Cronin, Chem. Commun. (2007) 468.

[11] (a) T.J.R. Weakley, H.T. Evans Jr., J.S. Showell, G.F. Tourné, C.M. Tourné, J. Chem. Soc. Chem. Commun. (1973) 139;
(b) R.G. Finke, M. Droege, J.R. Hutchinson, O. Gansow, J. Am. Chem. Soc. 103 (1981) 1587;
(c) S.H. Wasfi, A.L. Rheingold, G.F. Kokoszka, A.S. Goldstein, Inorg. Chem. 26 (1987) 2934;
(d) X. Zhang, Q. Chen, D.C. Duncan, R.J. Lachicotte, C.L. Hill, Inorg. Chem. 36 (1997) 4381;
(e) D. Drewes, E.M. Limanski, B. Krebs, Eur. J. Inorg. Chem. 44 (2005) 1542.

[12] (a) F. Robert, M. Leyrie, G. Hervé, Acta Crystallogr. B 38 (1982) 358;
(b) M. Bösing, A. Nöh, I. Loose, B. Krebs, J. Am. Chem. Soc. 120 (1998) 7252;
(c) T. Yamase, B. Botar, E. Ishikawa, K. Fukaya, Chem. Lett. (2001) 56;
(d) P. Mialane, J. Marrot, E. Rivière, J. Nebout, G. Hervé, Inorg. Chem. 40 (2001) 44;
(e) R.G. Finke, B. Rapko, T.J.R. Weakley, Inorg. Chem. 28 (1989) 1573;
(f) F. Xin, M.T. Pope, J. Am. Chem. Soc. 118 (1996) 7731;
(g) N. Laronze, J. Marrot, G. Hervé, Inorg. Chem. 42 (2003) 5857;
(h) J.M. Clemente-Juan, E. Coronado, A. Gaita-Ariño, C. Giménez-Saiz, H.U. Güdel, A. Sieber, R. Bircher, H. Mutka, Inorg. Chem. 44 (2005) 3389;
(i) P.T. Witte, S.R. Chowdhury, J.E. Elshof, D. Sloboda-Rozner, R.N.P.L. Alsters, Chem. Commun. (2005) 1206;
(j) L.H. Bi, U. Kortz, B. Keita, L. Nadjo, H. Borrmann, Inorg. Chem. 43 (2004) 8367.

[13] (a) L. Ruhlmann, J. Canny, R. Contant, R. Thouvenot, Inorg. Chem. 41 (2002) 3811;
(b) X. Zhang, T.M. Anderson, Q. Chen, C.L. Hill, Inorg. Chem. 40 (2001) 418;
(c) U. Kortz, N.K. Al-Kassem, M.G. Savelieff, N.A. Al Kadi, M. Sadakane, Inorg. Chem. 40 (2001) 4742;
(d) I.M. Mbomekalle, B. Keita, M. Nierlich, U. Kortz, P. Berthet, L. Nadjo, Inorg. Chem. 42 (2003) 5143.

[14] (a) H. Andres, J.M. Clemente-Juan, M. Aebersold, H.U. Güdel, E. Coronado, H. Bulttner, C. Kearly, J. Melero, R. Burriel, J. Am. Chem. Soc. 121 (1999) 10028;
(b) N. Casañ-Pastor, J. Bas-Serra, E. Coronado, G. Pourroy, L.C.W. Baker, J. Am. Chem. Soc. 114 (1992) 10380.

[15] (a) A. Tézé, G. Hervé, Inorg. Synth. 27 (1990) 85;
[b] J. Canny, A. Tézé, R. Thouvenot, G. Hervé, Inorg. Chem. 25 (1986) 2114;
(c) N.H. Nsouli, B.S. Bassil, M.H. Dickman, U. Kortz, B. Keita, L. Nadjo, Inorg. Chem. 45 (2006) 3858.

[16] (a) G.M. Sheldrick, SHELXS97, Program for Crystal Structure Solution, University of Göttingen, Germany, 1997;
(b) G.M. Sheldrick, SHELXL97, Program for Crystal Structure Refinement, University of Göttingen, Germany, 1997.

[17] Y.H. Wang, C.W. Hu, J. Peng, E.B. Wang, Y. Xu, J. Mol. Struct. 598 (2001) 161.

[18] The valence sum calculations are performed on a program of bond valence calculator, version 2.00 February (1993), written by C. Hormillosa with assistance from S. Healy, distributed by I.D. Brown.

[19] U. Kortz, S. Isber, M.H. Dickman, D. Ravot, Inorg. Chem. 39 (2000) 2915.

[20] J.J. Borrás-Almenar, J.M. Clemente-Juan, E. Coronado, B.S. Tsukerblat, J. Comput. Chem. 22 (2001) 985.